Mater. Res. Soc. Symp. Proc. Vol. 845 © 2005 Materials Research Society AA9.9

Selective Laser Sintering of Polycaprolactone Bone Tissue Engineering Scaffolds

Brock Partee[1], Scott J. Hollister[1,2] and Suman Das[1]
[1]Mechanical and [2]Biomedical Engineering Departments, University of Michigan
Ann Arbor, MI 48109-2125, U.S.A.

ABSTRACT

Present tissue engineering practice requires porous, bioresorbable scaffolds to serve as temporary 3D templates to guide cell attachment, differentiation, and proliferation. Recent research suggests that scaffold material and internal architecture significantly influence regenerate tissue structure and function. However, lack of versatile biomaterials processing methods have slowed progress towards fully testing these findings. Our research investigates using selective laser sintering (SLS) to fabricate bone tissue engineering scaffolds. Using SLS, we have fabricated polycaprolactone (PCL) and polycaprolactone/tri-calcium phosphate composite scaffolds. We report on scaffold design and fabrication, mechanical property measurements, and structural characterization via optical microscopy and micro-computed tomography.

INTRODUCTION

In the US, approximately a quarter of patients in need of organ transplants die while waiting for a suitable donor [1] and over 1.3 million surgical procedures are conducted every year to repair damaged or fractured bone [2]. The economic expense associated with tissue loss is estimated at more than $400 billion per year. Standard treatments include transplantation, surgical reconstruction, and the use of mechanical devices. However, problems resulting from the limited supply of donor organs, risk of rejection, and potential disease transmission have led to the investigation for alternative methods of treatment. Tissue engineering has the potential to resolve these areas of concern. It holds great promise for providing improved patient care and decreased health care costs by reducing the number of surgical procedures and recovery time associated with current medical practices.

Tissue engineering focuses on growing tissue from cells as opposed to making repairs using autografts, allografts, and prosthetics [2, 3]. It has been observed that isolated cells are unable to form mechanically and physiologically suitable neotissues if growth is left unassisted [4]. As a result, present tissue engineering practice generally requires the use of porous, bioresorbable scaffolds to serve as temporary, three-dimensional templates to guide cell attachment, differentiation, proliferation, and subsequent regenerate tissue formation. Recent research strongly suggests that the choice of scaffold material and its internal porous architecture significantly affect regenerate tissue type, structure, and function [5-6]. Image-based design techniques, such as those developed by Hollister et al. [7], have introduced the rapid design and analysis of biomimetic and periodic scaffold topologies that aim to simultaneously optimize scaffold architecture, material composition, and mechanical performance. The computational methods employed by these techniques address the conflicting design goals for tissue engineering scaffolds (i.e. need to create strong, stiff structures incorporating high levels of porosity). They typically generate very complex scaffold geometries that present enormous challenges in terms of both scaffold design and materials processing.

In this work we report on our use of Selective Laser Sintering (SLS) for constructing bone tissue engineering scaffolds. SLS is a laser-based solid freeform fabrication technique in which an object is built layer-by-layer using powdered materials, radiant heaters, and a computer controlled laser [8]. In SLS, the digital representation of an object is mathematically sliced into a number of thin layers. The object is then created by scanning a laser beam and selectively fusing (melting/sintering) patterns into sequentially deposited layers of a powder. Each patterned layer of powder is also fused to its underlying layer and corresponds to a cross-section of the object as determined from the mathematical slicing operation. This layered manufacturing method allows objects with a high degree of geometric complexity to be easily fabricated and enables the direct conversion of an object's computer model into its physical realization—allowing patient specific tissue reconstruction strategies to be easily developed.

EXPERIMENTAL DETAILS

Test specimens were fabricated using polycaprolactone (PCL) and inorganic particulate filled composites incorporating tri-calcium phosphate (TCP). These materials were chosen for the following reasons: (1) they are among the most widely investigated biocompatible, bioresorbable materials, (2) they are FDA approved biomaterials in common clinical use, and (3) they are readily available in powder form suitable for SLS processing. PCL powder marketed under the brand name CAPA® 6501 (Solvay Caprolactones, Warrington, UK) was used in this study. It is a semicrystalline (56%) aliphatic thermoplastic having a melting point of 58-60°C and a glass transition temperature of approximately -60°C [9]. Gel Permeation Chromatography (GPC) analysis (THF, 25°C) was conducted to determine the molecular weight of CAPA® 6501 both before and after processing (pre-processed PCL: $M_n = 91{,}900 \pm 7{,}700$; post-processed PCL: $M_n = 73{,}000 \pm 6{,}300$). Mechanical test sieving conducted according to ISO 2591-1 standards confirmed the powder to have an average particle size of 90μm and a distribution in which 98% of all particles are less than 125μm in size (no particles > 150μm). The TCP powder, chemical formula $Ca_5(PO_4)_3OH$, used in this study was obtained from Astaris LLC (St. Louis, MO). This particular powder (CAS NO. 1306-06-5) is a FCC grade TCP conditioner with an average particle size of 45μm and a broad distribution (no particles > 150μm). PCL/TCP powder mixtures were created by physically blending pure PCL and TCP powders in a rotary tumbling-mixer prior to SLS processing. Our preliminary investigations focused on processing pure PCL powder and 90-10 vol.% PCL/TCP powder blends. All powders were processed using a Sinterstation® 2000 commercial SLS machine (3D Systems Inc., Valencia, CA). Preheated and sequentially deposited powder layers were scanned using a low power continuous wave CO_2 laser (λ=10.6μm, power <10W) focused to a 450μm spot. The application of laser and thermal energy induced viscous sintering to take place, followed by rapid melting and resolidification of the polymer within and across adjacent powder layers to produce solid parts.

Two-level factorial design of experiments

A two-level factorial design of experiments (DOE) was conducted to analyze the effects of laser power, scan speed, scan spacing, part bed temperature, and powder layer delay time on resulting PCL part quality. Table 1 lists these parameters along with a brief description and the corresponding ranges that were investigated. Figure 1 outlines a schematic of the test geometry used in the DOE. It consists of a half-porous, half-solid cube that that replicates the typical

features and features sizes found in many bone tissue engineering scaffolds. The porous section is representative of many periodic pore scaffold architectures while the solid section is representative of surgical fixation base structures found in many scaffold designs.

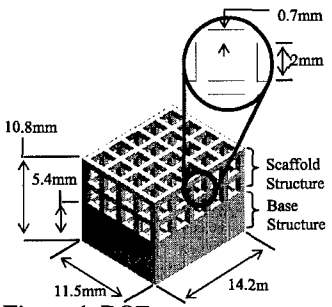

Figure 1. DOE test geometry

Table 1. SLS parameters and ranges investigated

Parameter	Description	Unit	Low Level	High Level
Laser power	Amount of laser power delivered during laser scanning	Watts	4.1	5.4
Scan speed	Speed of laser beam during scanning	mm/sec (in /sec)	1079.5 (42.5)	1231.9 (48.5)
Scan spacing	Distance between parallel laser scans	µm (in)	76.2* (0.003)	152.4 (0.006)
Part bed temp	Temperature of powder during laser scanning (monitored by IR sensor)	°C	46	48**
Powder layer delay	Exposure time of scanned section to radiant heater before new powder layer.	sec	0	8

SLS part quality was defined in terms of the following characteristics: (1) ease of part break-out, (2) degree of dimensional accuracy, and (3) the resulting void fraction content (i.e. level of process induced porosity). Ease of part break-out is a qualitative measure of the effort involved in removing the support powder surrounding a completed part. This characteristic was quantified by assigning a numerical value between 0 and 1 to each base and scaffold structure (0 – easy powder removal, 1 – difficult/impossible powder removal). Dimensional accuracy was determined by calculating the dimensional deviation (average percent difference) of measured part dimensions from that of their nominal design values. Base dimensions were measured using digital calipers and pore geometry was measured using a combination of optical microscopy and corresponding image analysis. The void fraction content for each test part was obtained by analyzing cross-sectional photomicrographs of each base and scaffold structure using ImageJ (http://rsb.info.nih.gov/ij/) image analysis software. Thresholding operations were used to isolate voids from the surrounding fully dense material matrix and a planar area-based void fraction analysis was conducted on each part.

Mechanical Testing

Tensile and compressive testing was conducted in accordance with ASTM standards D638-03 and D695-02a. Mechanical test specimens designed with solid and porous gage sections were fabricated by SLS using CAPA® 6501 PCL. Testing was conducted both parallel and perpendicular to the SLS build direction (i.e. across and along direction of layer stacking). The porous test specimens incorporated a network of 2mm x 2mm cubical channels in one, two, and three-dimensions. A schematic outlining the test geometries, dimensions, build orientation, and loading direction is shown in Figure 2. Tensile specimens were tested using a displacement controlled Instron 4206 tensile testing machine (Instron Corp., Canton, MA) at a displacement rate of 50 mm/min. Each specimen was loaded to failure or until the maximum allowable crosshead travel (433mm) was reached. Compression specimens were mechanically tested using a MTS Alliance RT30 test frame (MTS Systems Corp., Eden Prairie, MN). Specimens were compressed to 50% strain between two steel platens at a rate of 1 mm/min after an initial preload

of 6.7 N (1.5 lb) was applied. Tensile and compressive properties reported for specimens incorporating porous gage sections correspond to effective values of stress and strain.

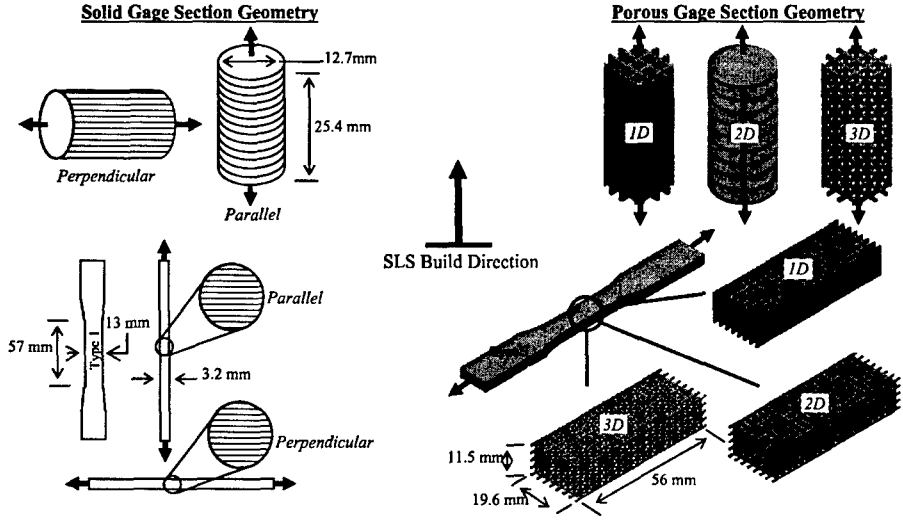

Figure 2. Mechanical test specimen geometry, build orientation, and loading direction

Micro-computed tomography structural characterization

One test specimen from each geometry type was scanned using a MS8X-130 Enhanced Vision Systems micro-computed tomography (μ-CT) machine (GE Medical Systems, Toronto, Canada) at a resolution of 28.1μm. GEMS Microview (GE Medical Systems, Toronto, Canada) was then used to threshold and analyze a representative region of interest (ROI) from each sample to determine the total (designed) porosity and level of manufacturing induced porosity (volume based void fraction analysis).

RESULTS AND DISCUSSION

Optimal SLS parameters for processing PCL

A mathematical model was developed that relates the influence of the five process parameters under investigation to resulting SLS part quality. Nonlinear programming using the *fmincon* function of Matlab software (The Mathworks Inc, Natick, MA), was used to optimize this process model to determine the set of optimal SLS parameters for processing PCL. Table 2 shows the optimal process parameter settings that were obtained. Parts fabricated at these settings were found to be easily removed from surrounding support powder, dimensionally accurate (within 3-8% of design specification), and near fully dense (>95%). Figures 3a and 3b show a picture of a DOE test part fabricated at these settings and a cross-sectional photomicrograph depicting its resulting microstructure respectively.

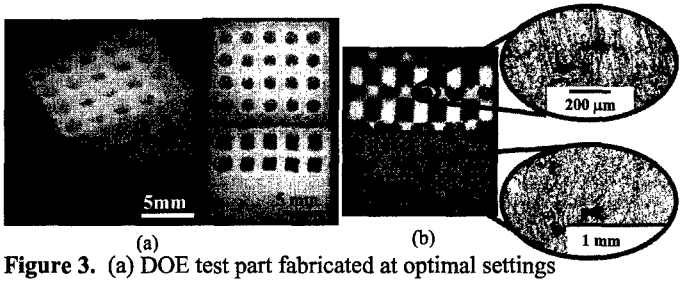

(a) (b)

Table 2. Optimal settings

Parameter	Setting	
	Base	Scaffold
Laser power	4.1 W	4.1 W
Scan speed	1079.5 mm/sec	1079.5 mm/sec
Scan spacing	152.4 μm	152.4 μm
Part bed temperature	46°C	46°C
Powder layer delay	0 sec	8 sec

Figure 3. (a) DOE test part fabricated at optimal settings
(b) Cross-section depicting microstructure of optimally processed PCL DOE test part

As a proof of concept, the optimal settings were used to fabricate actual minipig and human condyle scaffolds in PCL. Figure 4a shows a 3D rendition of a minipig mandibular condyle scaffold design and the corresponding PCL artifact. Figures 4b and 4c show the 3D rendition of two different human condyle scaffold designs and their corresponding PCL renditions. The scaffolds were designed using image-based design methods developed by *Hollister et al* [7]. The exterior geometry was derived from 3D reconstructions of actual bone CT images and a porous architecture was digitally superimposed in selected regions. These scaffolds incorporate complex external geometries and internal porous architectures having 700μm struts and 1.1-2mm pores.

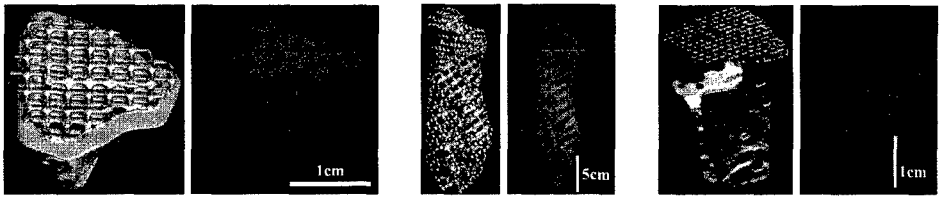

(a) (b) (c)

Figure 4. 3D renditions and actual SLS processed PCL scaffolds of (a) minipig mandibular condyle scaffold design and (b, c) two different human condyle scaffold designs

Mechanical and structural evaluation of optimally processed PCL

The mechanical property measurements for SLS processed PCL loaded both parallel (across layers) and perpendicular (along layers) to the build direction are listed in Table 3. These measurements provide baseline mechanical properties of bulk PCL and important information on the mechanical performance of porous PCL scaffold structures. Even though SLS processed PCL exhibits signs of anisotropy, it was found to be quite strong/stiff, having bulk mechanical properties comparable to those measured for PCL processed via injection molding and falling within the lower range measured for trabecular bone [10]. Figure 5 illustrates a representative volume-rendered μ-CT image of a porous compression test specimen (D695 3D). Table 4 lists the results of μ-CT structural analysis of PCL scaffolds processed by SLS and confirms that both solid and designed porous architecture sections are near fully dense.

Table 3. Mechanical property assessment of bulk and porous SLS processed PCL

	Property	Unit	SLS					Injection Molding[2]
			Solid Gage Section		Porous Gage Section[1]			
			//	⊥	1D	2D	3D	
Tension	Elastic Modulus, E	MPa	363.4 ± 71.6	343.9 ± 33.2	140.5 ± 19.6	42.0 ± 6.9	35.5 ± 5.8	430
	0.2% Offset Yield Strength, σ_Y	MPa	8.2 ± 1.0	10.1 ± 1.5	3.2 ± 0.6	0.67 ± 0.08	0.67 ± 0.06	17.5
	Strain at Yield, ε_Y	mm/mm	0.024 ± 0.006	0.031 ± 0.002	0.024 ± 0.001	0.017 ± 0.002	0.020 ± 0.002	---
	Ultimate Strength, σ_{UT}	MPa	---	16.1 ± 0.3	4.5 ± 0.4	1.2 ± 0.2	1.1 ± 0.1	--
	Strain at Break, ε_B	mm/mm	0.043 ± 0.007	> 7.90	0.095 ± 0.022	0.092 ± 0.022	0.096 ± 0.025	> 7
Compression	Elastic Modulus, E	MPa	299.0 ± 9.2	317.1 ± 3.9	133.4 ± 2.6	12.1 ± 0.5	14.9 ± 0.6	---
	0.2% Offset Yield Strength, σ_Y	MPa	12.5 ± 0.4	10.3 ± 0.2	4.25 ± 0.05	0.45 ± 0.01	0.42 ± 0.03	---
	Strain at Yield, ε_Y	mm/mm	0.052 ± 0.003	0.037 ± 0.002	0.0370 ± 0.000	0.0376 ± 0.001	0.0268 ± 0.003	---

[1]Porous compression specimens tested parallel to SLS build direction, porous tensile specimens tested perpendicular to SLS build direction
[2]Tests conducted at a strain rate of 100 mm/min

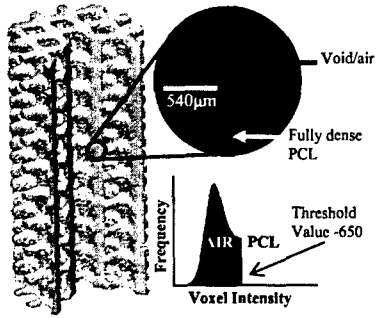

Table 4. μ-CT confirms SLS scaffolds near fully dense

	ASTM Specimen	Designed Porosity (%)			Process Induced Porosity (%)	% Fully Dense
		Measured[1]	Target[2]	Diff		
Solid	D638 //	Not Applicable			0.3	99.7
	D638 ⊥				0.9	99.1
	D695 //				0.4	99.6
	D695 ⊥				0.4	99.6
Porous	D638 1D	44.1	51.1	7.0	4.8	95.2
	D638 2D	57.5	68.5	11.0	2.6	97.4
	D638 3D	77.3	80.9	3.6	1.4	98.6
	D695 1D	44.8	56.9	12.1	2.9	97.1
	D695 2D	61.9	67.4	5.5	7.3	92.7
	D695 3D	76.5	83.3	6.8	3.4	96.6

[1]Calculated using GEMS Microview, [2]Calculated using Unigraphics

Figure 5. μ-CT volume-rendered porous test specimen along with close-up of resulting microstructure and thresholding histogram used to differentiate voids from fully dense PCL

PCL/TCP composite processing—preliminary results

SLS was used to fabricate monolithic and graded composition solid structures in PCL and 90-10 vol.% PCL/TCP blends(see figure 6). Such parts were found to exhibit excellent bonding within individual powder layers and across powder compositions. Subsequent μ-CT analysis showed these parts to be greater than 99.7% fully dense.

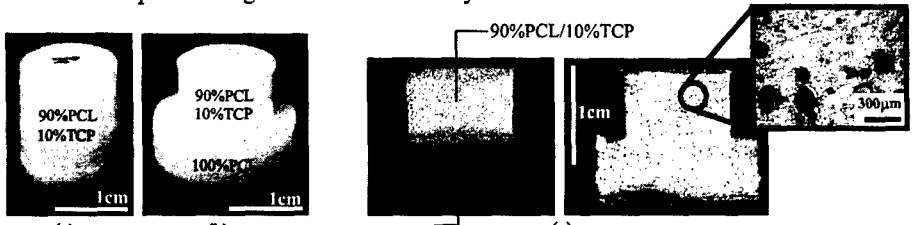

Figure 6. (a) uniform and (b) graded PCL/TCP cylinders and (c) resulting microstructure

CONCLUSIONS AND FUTURE WORK

The influence of SLS processing parameters including laser power, scan speed, scan spacing, part bed temperature, and powder layer delay time on overall part quality was investigated via a design of experiments approach. Optimal SLS parameters for processing PCL were developed to obtain dimensionally accurate, near fully dense bioresorbable tissue engineering scaffolds. SLS was used to fabricate monolithic and graded structures composed of PCL and 90-10 vol.% PCL/TCP powder blends. Excellent bonding was observed at the graded interface and such structures were found to be near fully dense as well. Future work will focus on further optimizing SLS processing of PCL/TCP blends. This will set the stage for development of SLS techniques capable of creating functionally tailored 3D scaffolds incorporating gradients in both material compositions and porosities which may assist physicians in simultaneously regenerating multiple different tissues (i.e. bone, cartilage, ligament, tendon).

ACKNOWLEDGEMENTS

This work is funded by the National Institute of Dental and Craniofacial Research (NIDCR) of the National Institutes of Health (NIH) under grant 5R21DE014736-02. The authors thank Bill Cook, Santy Sulaiman, and Colleen Flanagan for assistance with optical microscopy, GPC and μ-CT imagery. The authors gratefully acknowledge Astaris LLC for their TCP donation.

REFERENCES

1. U.S. Scientific Registry for Organ Transplantation and the Organ Procurement and Transplantation Network. Annual Report. Richmond, VA: UNOS, 1990.
2. R. Langer and J. Vacanti. "Tissue Engineering." Science. **260,** 920-926 (1993).
3. Griffith, Linda, and Gail Naughton. "Tissue Engineering—Current Challenges and Expanding Opportunities." Science. **295,** 1009-1014 (2002).
4. S. Yang, L. Kah-Fai, D. Zhaohui and C. Chee-Kai. "The Design of Scaffolds for Use in Tissue Engineering. Part I: Traditional Factors." Tissue Engineering. **7,** 679-689 (2001).
5. S.P. Bruder, K.H. Kraus, V.M. Goldberg, and S. Kadiyala. "Critical-Sized Canine Segmental Femoral Defects are Healed by Autologus Mesenchymal Stem Cell Therapy." Transactions of the 44th Annual Meeting of the Orthopedic Research Society. 147 (1998).
6. A.G. Mikos, G. Sarakinos, M.D. Lyman, D.E. Ingber, J.P. Vacanti, R. Langer. "Prevascularization of porous biodegradable polymer." Biotechnol. Bioeng. **42,** 716-723 (1993).
7. S.J. Hollister, R.D. Maddox, J.M. Taboas. "Optimal Design and Fabrication of Scaffolds to Mimic Tissue Properties and Satisfy Biological Constraints." Biomaterials. **23,** 4095-4103 (2002).
8. C.R. Deckard, "Selective Laser Sintering.", Ph.D. thesis, University of Texas at Austin, 1988.
9. Properties & Processing of CAPA® Thermoplastics. Solvay Caprolactones. Issue 1. (April 2001).
9. R.W. Goulet, S.A. Goldstein, M.J. Ciarelli, J.L. Kuhn, M.B. Brown, and L.A. Feldkamp. "The relationship between the structural and orthogonal compressive properties of trabecular bone." J Biomechanics. **27,** 375-389 (1994).